OAK RIDGE NATIONAL LABORATORY
operated by
UNION CARBIDE CORPORATION
NUCLEAR DIVISION
for the
U.S. ATOMIC ENERGY COMMISSION

ORNL- TM- 2043

EFFECTS OF IRRADIATION ON THE MECHANICAL PROPERTIES OF TWO VACUUM-MELTED HEATS OF HASTELLOY N

H. E. McCoy, Jr.

ORNL-TM-2043

Contract No. W-7405-eng-26

METALS AND CERAMICS DIVISION

EFFECTS OF IRRADIATION ON THE MECHANICAL PROPERTIES OF TWO VACUUM-MELTED HEATS OF HASTELLOY N

H. E. McCoy, Jr.

JANUARY 1968

OAK RIDGE NATIONAL LABORATORY
Oak Ridge, Tennessee
operated by
UNION CARBIDE CORPORATION
for the
U.S. ATOMIC ENERGY COMMISSION

TABLE OF CONTENTS

EFFECTS OF IRRADIATION ON THE MECHANICAL PROPERTIES OF TWO VACUUM-MELTED HEATS OF HASTELLOY N

H. E. McCoy, Jr.

ABSTRACT

The mechanical behavior of two vacuum-melted heats of Hastelloy N was evaluated at 650 and 760°C. The material was subjected to several thermal-mechanical treatments and then irradiated at 650 and 760°C to a thermal dose of 2.3×10^{20} neutrons/cm^2. The results are compared with those for unirradiated specimens that were given a similar thermal treatment. The various thermal-mechanical treatments had some relatively small effects on the unirradiated tensile properties, but the creep properties were very similar. The primary effects of irradiation were reductions in the creep-rupture life and the rupture ductility in both creep and tensile tests. These observations are explained on the basis of helium production in the metal by the $^{10}B(n,\alpha)$ transmutation.

INTRODUCTION

The potential use of Hastelloy N in several reactors has developed considerable interest in how the properties of this material change with neutron irradiation. Previous studies at ORNL[1,2] have shown that the high-temperature mechanical properties of this alloy deteriorate under neutron irradiation. This deterioration manifests itself as both a reduction in the creep-rupture life and in the rupture ductility. However, these studies involved air-melted material with B levels in the range of 20 to 50 ppm.

---

[1]W. R. Martin and J. R. Weir, Nucl. Appl. 1(2), 160–167 (1965).

[2]W. R. Martin and J. R. Weir, Nucl. Appl. 3(3), 167–177 (1967).

We have recently run two series of experiments that were aimed primarily at characterizing this alloy for use in the SNAP-8 system. This system will utilize thin-walled Hastelloy N tubing for fuel element cladding and will operate over the temperature range of 650 to 760°C. One series of experiments involved in-reactor tube-burst tests on cladding material, and the details of this study have been reported.[3] The second series of experiments involved postirradiation creep rupture and tensile tests on small bar samples, and these results are presented in this report. Two vacuum-melted heats were used, and the properties were evaluated after the material had been subjected to various thermal-mechanical treatments. These treatments were dictated largely by the steps used to process the fuel element cladding.

EXPERIMENTAL DETAILS

Test Materials

The two lots of material used in this study were 12-in.-diam, 10,000-lb double vacuum-melted heats obtained from Allvac Metals Company. The chemical analysis of each heat is given in Table 1. Heat 5911 was obtained in two forms: forged to a bar 2 x 2 in. (designated 5911 AW) and forged and machined to a tube shell 2-in. OD x 1 1/2-in. ID (designated 5911 TH). Heat 6252 was obtained in the as-cast condition (designated 6252 AC).

Heat Treatments

The materials were given several different mechanical and thermal treatments prior to irradiation. These treatments are described in Table 2 and will be referred to by number. All annealing was carried out in an argon environment, and the specimens were cooled by pulling them into a water-cooled section at the end of the furnace.

---

[3]H. E. McCoy, Jr., and J. R. Weir, In- and Ex-Reactor Stress-Rupture Properties of Hastelloy N Tubing, ORNL-TM-1906 (September 1967).

Table 1. Chemical Analysis of Test Materials

Element	Content (wt %)	
	Heat Number 5911	Heat Number 6252
Fe	0.03	0.12
Cr	6.14	7.26
Mo	17.01	16.53
Ni	bal	bal
C	0.056	0.051
Mn	0.21	0.20
B	0.0010	0.0003
S	0.002[a]	0.002[a]
P	0.002[a]	0.002[a]
Si	0.05	0.05
Cu	< 0.01	< 0.01
Co	0.08[a]	0.11[a]
Al	0.15	0.20
Ti	0.067	0.13
W	0.01[a]	0.02[a]
Zr	< 0.01	< 0.01
O	0.0014	0.0008
N	< 0.0005	0.0005

[a]Ladle analysis, Allvac Metals Company.
All other values obtained at ORNL on the finished product.

Test Specimen

The small tensile specimen shown in Fig. 1 was used for in- and ex-reactor tests. The small size made it possible to get several specimens into a single experiment. Our work with this specimen has shown that it yields data that are quite similar to those obtained from larger specimens. Because of the stress concentration at the base of the filet, there is some tendency for the brittle specimens to fail at this point.

Irradiation Conditions

The specimens were irradiated in a single-test capsule in the P-4 poolside position in the ORR. The peak thermal flux was 6×10^{13} neutrons cm^{-2} sec^{-1}, and the peak fast (> 2.9 Mev) flux was 5×10^{12} neutrons cm^{-2} sec^{-1}. The duration of the experiment was 1080 hr

Table 2. Description of Thermal-Mechanical Treatments

Designation	Thermal-Mechanical Treatment
1	Annealed 1 hr at 1177°C in argon
2	Hot rolled 50% at 1150°C, Annealed 1 hr at 1177°C in argon
3	Annealed 1 hr at 1177°C in argon, Cold worked 25%, Annealed 1 1/2 hr at 1066°C in argon, Annealed 2 hr at 1093°C in argon, Annealed 10 min at 1150°C in argon
3A	Annealed 1 hr at 1260°C in argon
2A	Hot rolled 50% at 1150°C, Annealed 1 hr at 1260°C in argon

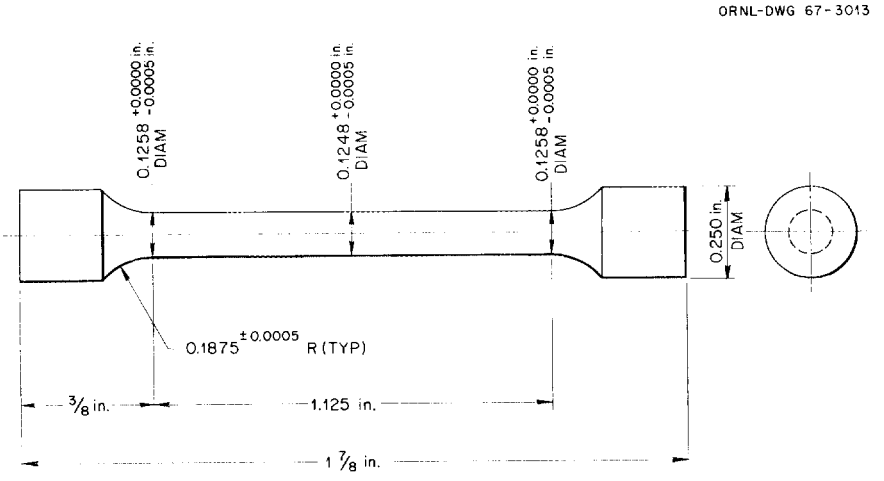

Fig. 1. Test Specimen

(time at temperature and full power), so the thermal and fast doses were 2.3×10^{20} and 1.9×10^{19} neutrons/cm^2, respectively. Each specimen was heated by a small furnace, and the temperature was controlled by a proportioning controller which acted on response to a Chromel-P–Alumel thermocouple attached to the specimen gage length. Some of the specimens were controlled at 650°C, but most of them were held at 760°C. The environment in the capsule was flowing He–1% O_2. Ex-reactor control specimens were given the same thermal exposure as the in-reactor specimens.

Testing Techniques

The laboratory creep-rupture tests were run in conventional creep machines of the dead load and lever arm types. The strain was measured by a dial indicator that showed the total movement of the specimen and part of the load train. The zero strain measurement was taken immediately after the load was applied. The temperature accuracy was ±0.75%, the guaranteed accuracy of the Chromel-P–Alumel thermocouples used.

The postirradiation creep-rupture tests were run in lever arm machines that were located in hot cells. The strain was measured by an extensometer with rods attached to the upper and lower specimen grips. The relative movement of these two rods was measured by a linear differential transformer, and the transformer signal was recorded. The accuracy of strain measurements is difficult to determine. The extensometer (mechanical and electrical portions) produced measurements that could be read to about ±0.02% strain. However, other factors (temperature changes in the cell, mechanical vibrations, etc.) probably combined to give an overall accuracy of ±0.1% strain. This is considerably better than the specimen-to-specimen reproducibility that one would expect for relatively brittle materials. The temperature measuring and control system was the same as that used in the laboratory with one exception. In the laboratory, the control system was stabilized at the desired temperature by use of a recorder with an expanded scale. In the tests in the hot cells, the control point was established by setting the controller without the aid of the expanded-scale recorder. This error and the thermocouple accuracy combine to give a temperature uncertainty of about ±1%.

The tensile tests were run on Instron Universal Testing Machines. The strain measurements were taken from the crosshead travel.

The test environment was air in all cases. Metallographic examination showed that the depth of oxidation was small (< 0.002 in.), and hence, we feel that the environment did not appreciably influence the test results.

Experimental Results

The results of tensile tests run on the materials in this study are summarized in Tables 3 and 4. All of the unirradiated specimens were subjected to a thermal aging treatment (1080 hr at 650 or 760°C) equivalent to that of the irradiated specimens. The data in Table 3 indicate several important features of the tensile properties of the unirradiated materials.

1. The yield stress decreases slightly with increasing test temperature, whereas the tensile stress decreases by about a factor of 2 over the temperature range of 550 to 760°C.
2. There appear to be some small variations in the yield and tensile strengths due to the various heat treatments. For example, the data for heat 5911 AW-anneal 1 indicate that aging at 650°C results in lower yield stress and a higher tensile stress than aging at 760°C. The anneals at 1260°C (3A and 2A) cause slight strength reductions.
3. The fracture ductility decreases with increasing test temperature for all materials.
4. The data for 5911 AW-anneal 1 indicate that aging at 650°C results in better ductility than aging at 760°C.
5. A comparison of the data for 5911 AW-anneals 1 and 3 indicate that the ductility of the materials receiving the anneal 3 is lower when aged and tested at 650°C and higher at 760°C.
6. Heat 6252 AC generally exhibited lower ductility than heat 5911. This is probably due to the smaller amount of working received by heat 6252 AC. This is supported

Table 3. Tensile Properties of Unirradiated Materials[a]

Anneal[b]	Specimen Number	Test Temperature (°C)	Stress (psi)		Elongation (%)		Reduction in Area (%)	Pretest Aging[c]
			Yield	Tensile	Uniform	Total		
			Heat 5911 AW					
1	3113	550	32,600	87,800	57.1	58.2	41.6	2
1	3114	600	35,400	65,200	22.5	23.5	23.2	2
1	3109	760	32,200	47,700	8.0	13.4	14.4	2
1	3115	760	31,700	51,100	12.8	16.6	13.1	2
1	3117	550	31,400	96,500	61.7	64.8	47.5	1
1	3108	650	29,700	77,700	39.8	40.8	35.3	1
1	3121	760	28,900	50,900	12.5	25.9	27.3	1
3A	3106	650	26,400	70,800	43.2	43.4	36.6	1
3A	2854	760	31,700	46,700	8.0	13.6	12.5	2
3	2959	650	34,300	76,600	29.6	30.3	25.7	1
3	2953	760	32,200	45,800	8.2	22.9	22.1	2
			Heat 5911 TH					
1	3103	650	29,200	74,300	41.1	42.7	33.5	1
1	3091	760	32,400	47,800	7.7	16.2	13.9	2
			Heat 6252 AC					
2	2919	650	34,000	66,600	15.1	15.4	17.4	1
2	2921	760	32,000	45,000	6.1	8.6	7.3	2
2 + 3	2948	650	37,100	73,500	21.6	21.9	19.1	1
2 + 3	2944	760	33,500	44,700	8.7	20.2	17.6	2
2A	3130	760	25,700	46,800	7.7	10.6	10.1	2

[a] At a strain rate of 0.002 min^{-1}.

[b] Anneal designation given in Table 2.

[c] 1 – 1080 hr at 650°C; 2 – 1080 hr at 760°C.

Table 4. Tensile Properties of Irradiated Materials[a]

Heat Number	Anneal	Specimen Number	Temperature (°C)		Stress (psi)		Elongation (%)		Reduction in Area (%)
			Irradiation	Test	Yield	Tensile	Uniform	Total	
5911 AW	1	2837	760	760	32,600	32,700	1.0	1.0	3.6
5911 AW	1	2839	760	760	33,700	33,700	1.1	1.4	2.0
5911 AW	1	2846	650	650	38,200	50,600	7.7	8.1	11.2
5911 AW	1	2847	650	650	36,400	52,600	10.5	11.2	14.6
6252 AC	2	2917	760	760	32,200	32,200	1.1	1.5	0.9
6252 AC	2	2918	760	760	31,800	31,800	1.2	1.5	0.0
6252 AC	2	2926	650	650	39,100	48,500	4.6	4.8	5.6
6252 AC	2	2927	650	650	40,200	48,900	4.6	5.6	8.0

[a]Thermal dose equals 2.3×10^{20} neutrons/cm^2; strain rate equals 0.002 min^{-1}.

by the fact that the additional working received in the 2 + 3 treatment improved the ductility over that obtained after just the treatment 2.

The tensile properties of some of the materials were obtained at 650 and 760°C after irradiation, and these results are given in Table 4. A comparison of these data with those for the unirradiated specimens in Table 3 leads to several important observations:

1. The yield stress at 650°C is higher for the irradiated specimens whereas the yield stress at 760°C is equivalent for irradiated and unirradiated specimens.
2. The tensile stress is lower for the irradiated materials at both 650 and 760°C.
3. The ductility at both temperatures is reduced severely by irradiation, the reduction being much greater at 760°C.

The variations in the rupture ductility of Hastelloy N in the various conditions investigated are summarized in Fig. 2. The spread in the rupture

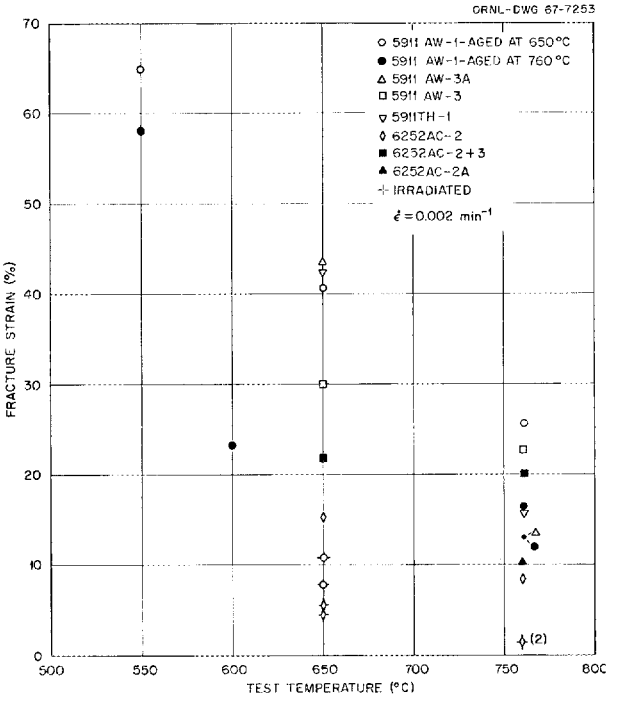

Fig. 2. Variation of the Tensile Fracture Strain with Temperature. (Unless designated otherwise, specimens were irradiated or aged at the test temperature.)

strain at a given test temperature is quite large. At 650°C, for example, the unirradiated material shows a range of about 15 to 44%, and the range is further extended by values as low as 5% in the irradiated condition.

The main emphasis in this study was on the creep-rupture properties, since the potential application involves service under creep conditions. The results of tests on unirradiated and irradiated specimens are given in Tables 5 and 6, respectively. The data on unirradiated materials are of value themselves, but we are more concerned with how the properties change as a result of irradiation. Figure 3 shows that the rupture ductility varies from about 15 to 30% for the unirradiated material at 650°C. However, many of the variations appear to be random rather than due to the effects of a particular pretest heat treatment. The general trend seems to be for decreasing ductility with increasing rupture life. Figure 4 compares the rupture lives of unirradiated and irradiated specimens at 650°C. The line for the irradiated material is based on our results for several air-melted heats. The results on the present heat at 650°C are inadequate to establish a stress-rupture curve, but the data are in reasonable agreement with those for the air melts. The rupture life variations appear to be entirely random with respect to material and conditions of annealing. The rupture life is reduced by an order of magnitude by irradiation, but there is some indication that this factor decreases with increasing rupture life. The minimum creep rate is shown in Fig. 5 as a function of the stress at 650°C for irradiated and unirradiated materials. The variation due to heat and anneal is again random and irradiation does not have any appreciable effect.

The rupture strain at 760°C is shown in Fig. 6 as a function of rupture life for unirradiated material. The rupture strain varies from 10 to 50% with most of the variation appearing to be independent of heat and annealing treatment. Most of the materials exhibit a trend of increasing strain with increasing rupture life. The rupture lives of the irradiated and unirradiated materials are compared in Fig. 7. Again, the variations due to heat and anneal appear to be random. One exception may be heat 6252 AC, which, after irradiation, has a greater rupture life. At a stress level of 20,000 psi, the rupture life is reduced about two orders of magnitude by irradiation. The curves converge

Table 5. Creep-Rupture Properties of Unirradiated Materials

Heat Number	Anneal[a]	Test Number	Test Temperature (°C)	Stress (psi)	Minimum Creep Rate (%/hr)	Rupture Life (hr)	Rupture Strain (%)	Reduction in Area (%)	Pretest Aging[b]
5911 AW	1	6185	650	65,000	0.590	9.4	26.5	21.9	1
5911 AW	1	6014	650	55,000	0.140	49.6	27.4	21.2	1
5911 AW	1	6013	650	47,000	0.043	206.5	17.3	17.1	1
5911 AW	1	6012	650	40,000	0.022	413.7	17.3	16.7	1
5911 AW	1	6186	650	40,000	0.018	598.2	22.7	11.0	1
5911 AW	1	6059	650	32,400	0.0045	1828.1	21.8	19.8	1
5911 AW	1	6126	760	30,000	0.83	21.8	29.8	23.1	2
5911 AW	1	6187	760	25,000	0.36	53.7	31.9	13.9	2
5911 AW	1	6023	760	20,000	0.12	147.7	35.5	20.6	2
5911 AW	1	6039	760	17,500	0.049	367.7	24.3	10.6	2
5911 AW	1	6024	760	15,000	0.035	607.2	39.8	29.0	2
5911 AW	1	6188	760	13,000	0.017	1198.9	29.7	16.0	2
5911 AW	3A	6057	650	47,000	0.026	120.8	27.2	21.1	1
5911 AW	3A	6015	650	40,000	0.012	489.0	21.0	17.3	1
5911 AW	3A	6040	760	30,000	0.94	15.4	23.6	16.1	2
5911 AW	3A	6025	760	20,000	0.14	114.7	24.6	16.1	2
5911 AW	3A	6026	760	15,000	0.025	402.8	13.3	8.0	2
5911 AW	3	6058	650	47,000	0.067	181.0	23.5	20.7	1
5911 AW	3	6016	650	40,000	0.025	761.7	29.5	22.8	1
5911 AW	3	6127	760	30,000	1.18	24.2	38.5	33.0	2
5911 AW	3	6189	760	25,000	0.42	47.0	34.4	15.0	2
5911 AW	3	6027	760	20,000	0.19	73.7	17.6	21.7	2
5911 AW	3	6041	760	17,500	0.13	153.3	29.3	17.3	2
5911 AW	3	6028	760	15,000	0.048	419.2	32.2	16.4	2
5911 TH	1	6042	650	55,000	0.018	48.9	27.9	21.6	1
5911 TH	1	6018	650	47,000	0.038	189.1	26.6	21.9	1
5911 TH	1	6017	650	40,000	0.023	706.3	29.2	25.4	1
5911 TH	1	6056	650	32,400	0.0019	2082.1	18.7	13.4	1
5911 TH	1	6125	760	30,000	0.765	17.7	19.2	14.3	2

Table 5 (continued)

Heat Number	Anneal[a]	Test Number	Test Temperature (°C)	Stress (psi)	Minimum Creep Rate (%/hr)	Rupture Life (hr)	Rupture Strain (%)	Reduction in Area (%)	Pretest Aging[b]
5911 TH	1	6190	760	25,000	0.41	27.7	14.1	10.7	2
5911 TH	1	6029	760	20,000	0.13	113.5	25.3	16.2	2
5911 TH	1	6043	760	17,500	0.054	161.4	11.9	10.0	2
5911 TH	1	6030	760	15,000	0.026	654.7	24.8	13.2	2
6252 AC	2	6022	650	47,000	0.054	99.3	9.4	12.2	1
6252 AC	2	6019	650	40,000	0.026	647.3	21.2	15.6	1
6252 AC	2	6060	650	32,400	0.0041	1813.3	15.9	14.7	1
6252 AC	2	6124	760	30,000	1.37	7.3	14.1	10.2	2
6252 AC	2	6191	760	25,000	0.51	48.9	31.2	14.3	2
6252 AC	2	6031	760	20,000	0.19	119.1	39.0	29.0	2
6252 AC	2	6044	760	17,500	0.13	130.8	22.5	15.7	2
6252 AC	2	6032	760	15,000	0.049	636.5	46.7	37.7	2
6252 AC	2A	6033	760	20,000	0.13	162.9	35.6	21.9	2
6252 AC	2A	6034	760	10,000	0.0047	3570.2	28.0	13.7	2
6252 AC	2 + 3	6021	650	47,000	0.073	123.6	17.5	13.9	1
6252 AC	2 + 3	6020	650	40,000	0.024	622.2	14.9	14.0	1
6252 AC	2 + 3	6045	760	30,000	0.80	10.0	13.1	12.0	2
6252 AC	2 + 3	6047	760	20,000	0.24	114.3	53.1	31.6	2
6252 AC	2 + 3	6046	760	15,000	0.044	535.6	46.6	21.6	2

[a]Anneal designation given in Table 2.

[b]1 – 1080 hr at 650°C; 2 – 1080 hr at 760°C.

Table 6. Creep-Rupture Properties of Irradiated Materials[a]

Heat Number	Anneal[b]	Test Number	Test and Irradiation Temperature (°C)	Stress (psi)	Minimum Creep Rate (%/hr)	Rupture Life (hr)	Rupture Strain (%)	Reduction in Area (%)	Specification Number	Comments
5911 AW	1	R-194	650	47,000	0.056	12.8	1.68	-0.9	2851	
5911 AW	1	R-182	650	40,000	0.015	43.0	0.83	8.2	2850	
5911 AW	1	R-170	650	32,400	0.0049	144.3	0.84	-4.0	2848	c
5911 AW	1	R-177	760	10,000	0.0086	104.6	0.98	-0.3	2842	
5911 AW	1	R-196	760	8,000	0.0011	834.8	1.77	0.0	2841	
5911 AW	3A	R-183	760	15,000	0.22	2.2	0.57	0.8	2849	
5911 AW	3A	R-201	760	10,000	0.0041	179.4	1.08	1.1	2845	
5911 AW	3	R-175	760	20,000	0.85	0.5	0.58	-1.5	2950	
5911 AW	3	R-180	760	10,000	0.011	55.2	1.34	4.5	2951	c
5911 AW	3	R-223	760	8,000	0.0024	825.7	4.49	0.0	2949	
5911 TH	1	R-176	760	20,000	0.28	1.0	0.67	3.1	2981	
5911 TH	1	R-184	760	15,000	0.090	2.1	0.99	-0.3	2980	
5911 TH	1	R-218	760	8,000	0.0024	365.2	1.45		2982	
6252 AC	2	R-197	650	47,000	0.021	16.8	1.50	-0.4	2937	
6252 AC	2	R-181	650	40,000	0.029	23.5	0.93	1.1	2929	
6252 AC	2	R-173	650	32,400	0.0050	220.6	1.70	-0.3	2928	c
6252 AC	2	R-185	760	15,000	0.18	3.5	0.95	0.0	2920	
6252 AC	2	R-224	760	12,500	0.039	24.1	1.55	4.8	2923	
6252 AC	2	R-178	760	10,000	0.0032	581.5	2.36	-1.8	2922	
6252 AC	2A	R-186	760	15,000	0.36	0.7	0.32	-2.2	2930	c
6252 AC	2A	R-217	760	10,000	0.0028	289.8	1.12	-3.7	2932	c
6252 AC	2 + 3	R-187	760	15,000	0.17	5.0	1.49	2.5	2939	
6252 AC	2 + 3	R-225	760	12,500	0.0067	284.3	3.18		2941	
6252 AC	2 + 3	R-209	760	10,000	0.0046	504.6	3.58	3.5	2940	

[a] Dose equals 2.3×10^{20} neutrons/cm^2.

[b] Anneal designation given in Table 2.

[c] Specimen broke in the radius at the end of gage section.

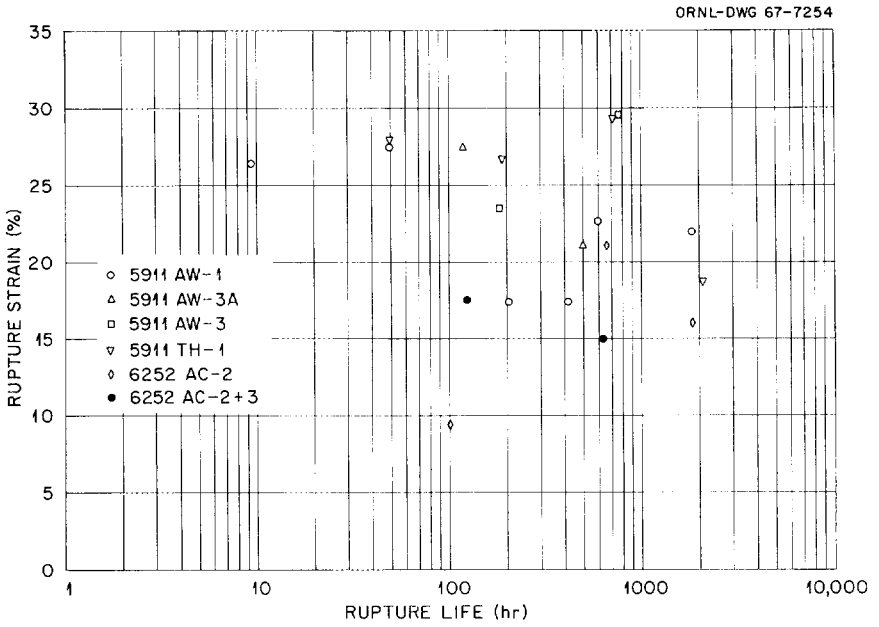

Fig. 3. Variation of the Rupture Strain with Rupture Life Under Creep at 650 °C.

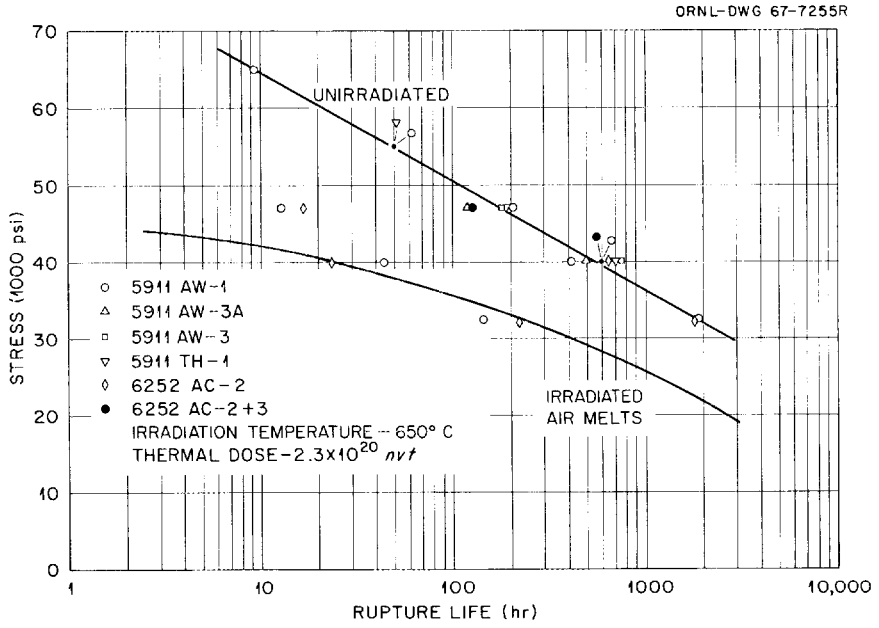

Fig. 4. A Comparison of the Creep-Rupture Properties of Irradiated and Unirradiated Hastelloy N at 650 °C.

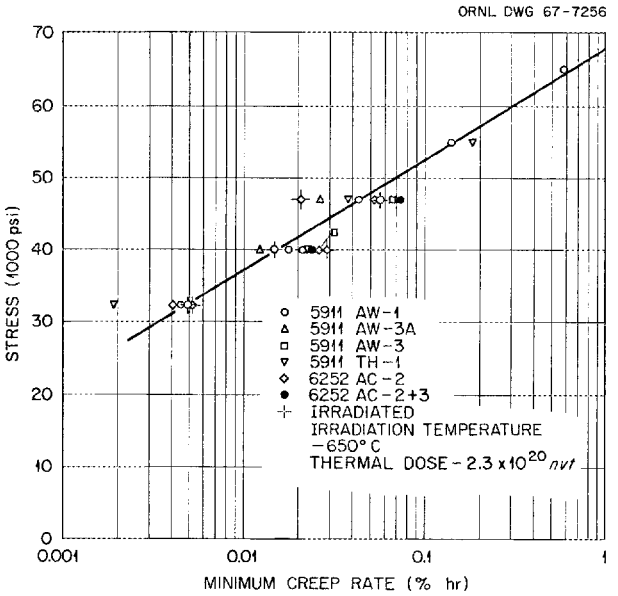

Fig. 5. A Comparison of the Creep Rates of Irradiated and Unirradiated Hastelloy N at 650°C.

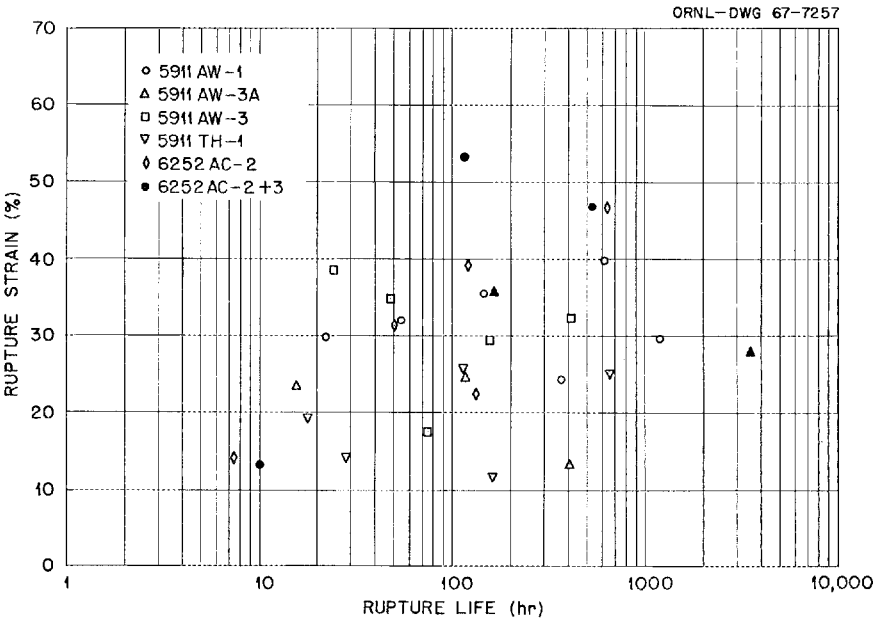

Fig. 6. The Variation of Rupture Strain with Creep-Rupture Life for Hastelloy N at 650°C.

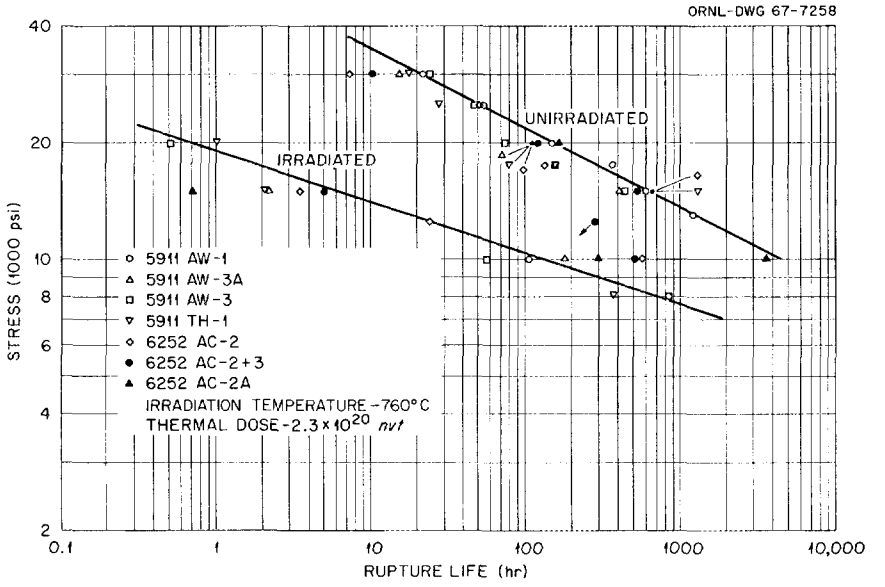

Fig. 7. A Comparison of the Creep-Rupture Properties of Irradiated and Unirradiated Hastelloy N at 760°C.

slightly as the stress level is reduced. The minimum creep rates of the irradiated and unirradiated specimens are compared in Fig. 8. At a stress level of 20,000 psi, the creep rate of the irradiated material is higher. As the stress is decreased, the curves converge to where the difference in creep rate below 10,000 psi is negligible.

The rupture strains of the irradiated specimens are compared in Fig. 9 as a function of strain rate. Although the tensile tests at a strain rate of 0.002 min^{-1} (12%/hr) indicated that the ductility was much lower at 760°C than at 650°C, the ductility appears to be independent of temperature at strain rates below about 0.1%/hr. There is also a distinct trend of increasing fracture strain with decreasing strain rate.

Although all of the creep curves were examined in detail, only a few typical ones will be presented. The data were taken manually, but were reduced and plotted by computer. Figures 10, 11, 12, and 13 are direct photographs of the plotted data after the curves were drawn in manually. Figures 10 and 11 show the results of tests on unirradiated and irradiated specimens, respectively, from heat 5911 AW-anneal 1 at 650°C and 40,000 psi. The primary creep stage is very short, and the accumulated strain at the beginning of secondary creep was only about 0.1%. A comparison of points on the two plots indicates that the results

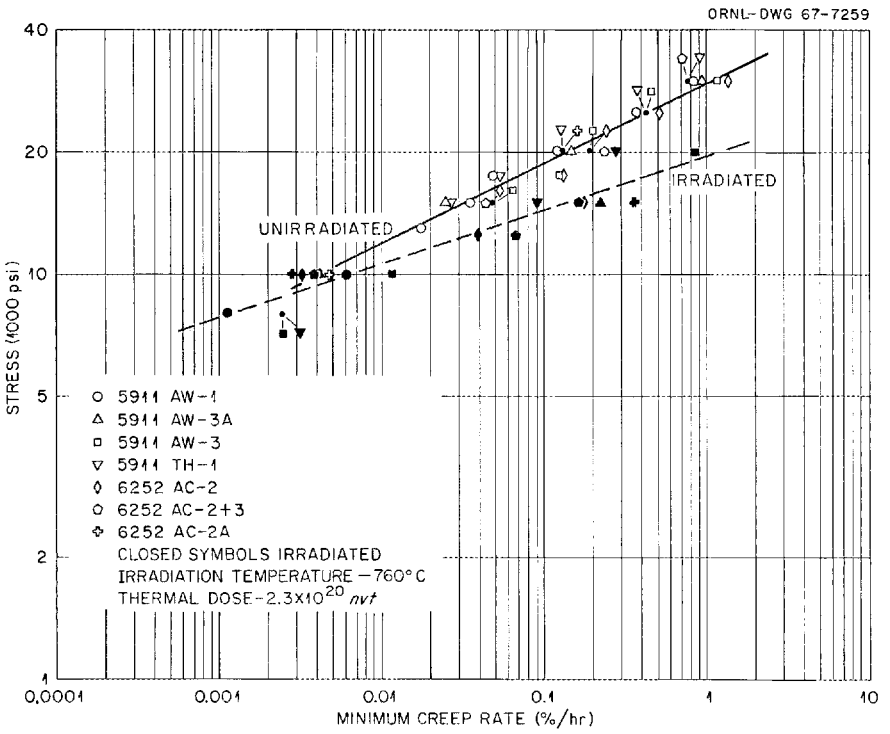

Fig. 8. A Comparison of the Creep Rates of Irradiated and Unirradiated Hastelloy N at 760 °C.

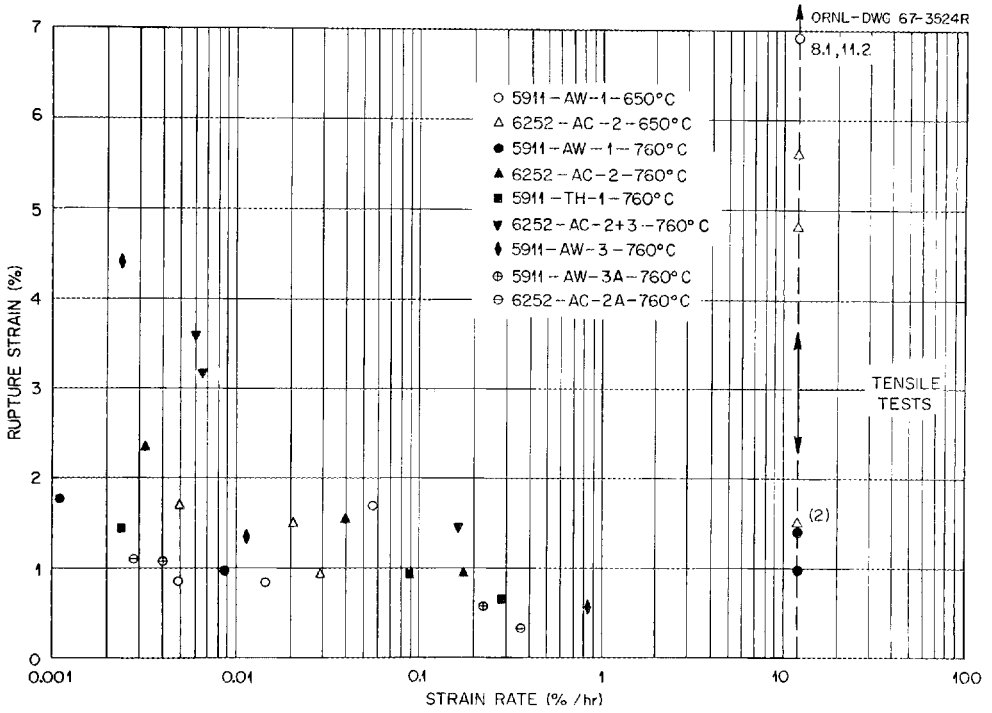

Fig. 9. Fracture Ductilities for Hastelloy N Under Several Test Conditions.

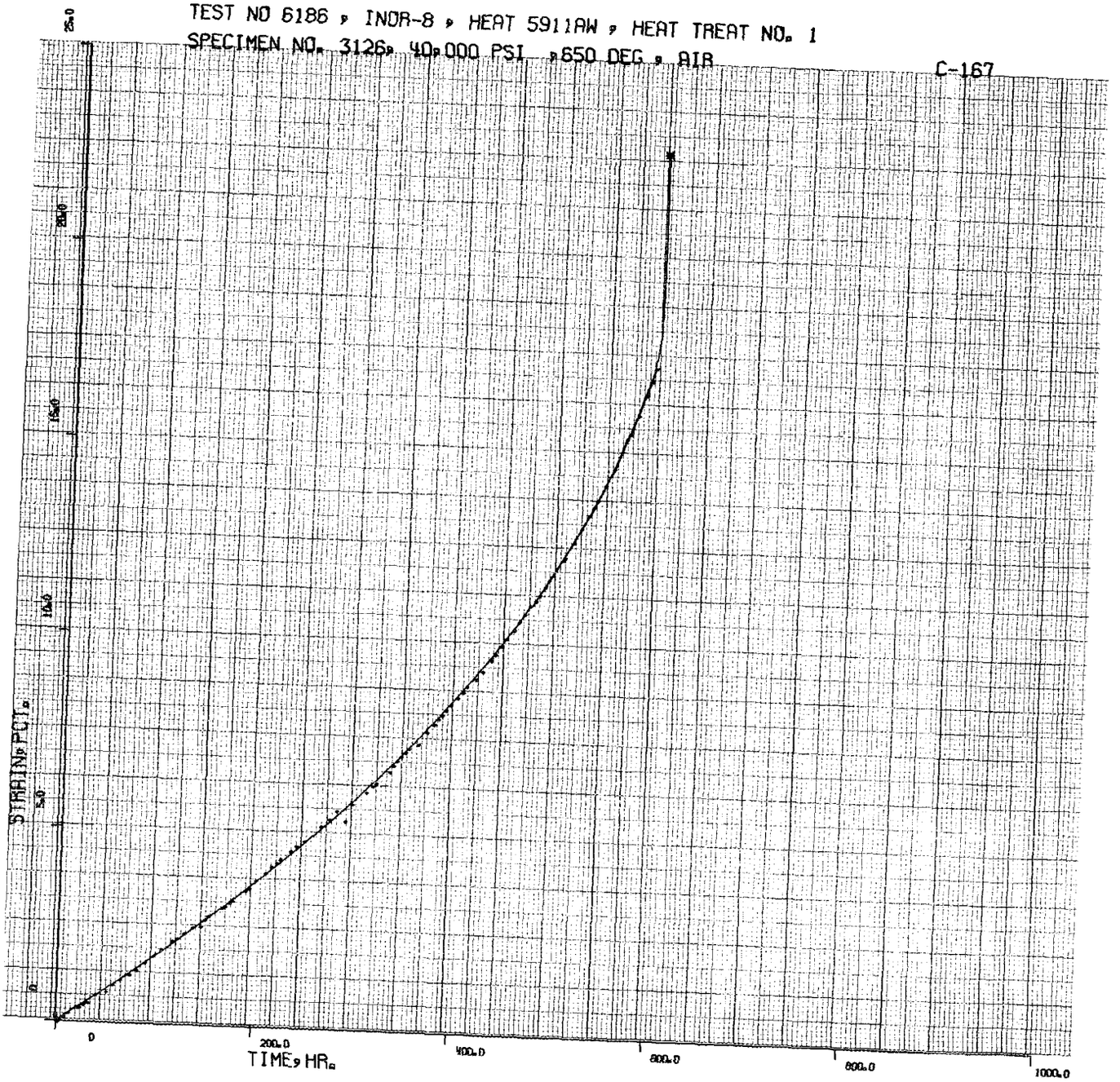

Fig. 10. Creep Curve for Test 6186.

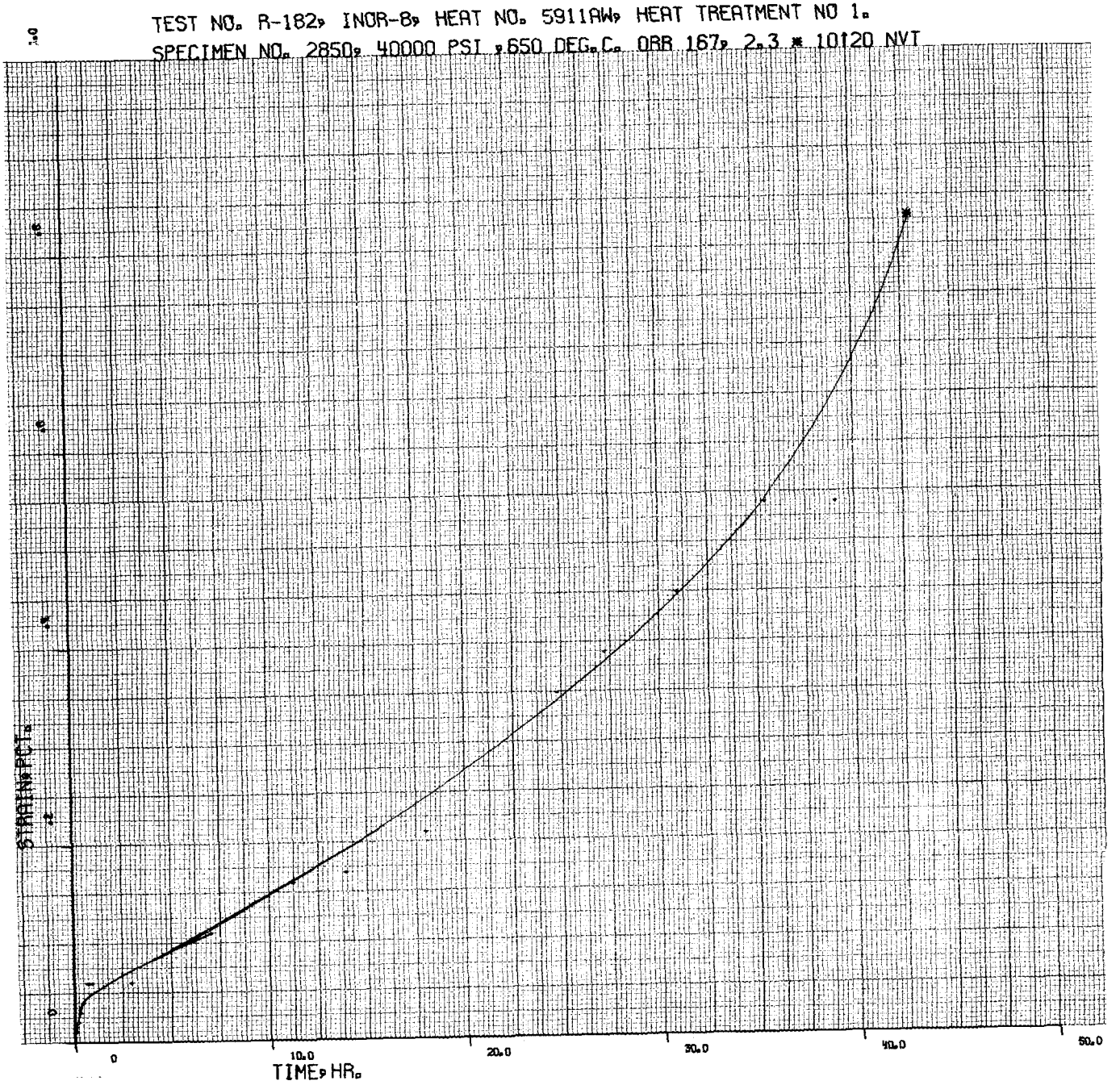

Fig. 11. Creep Curve for Test R-182.

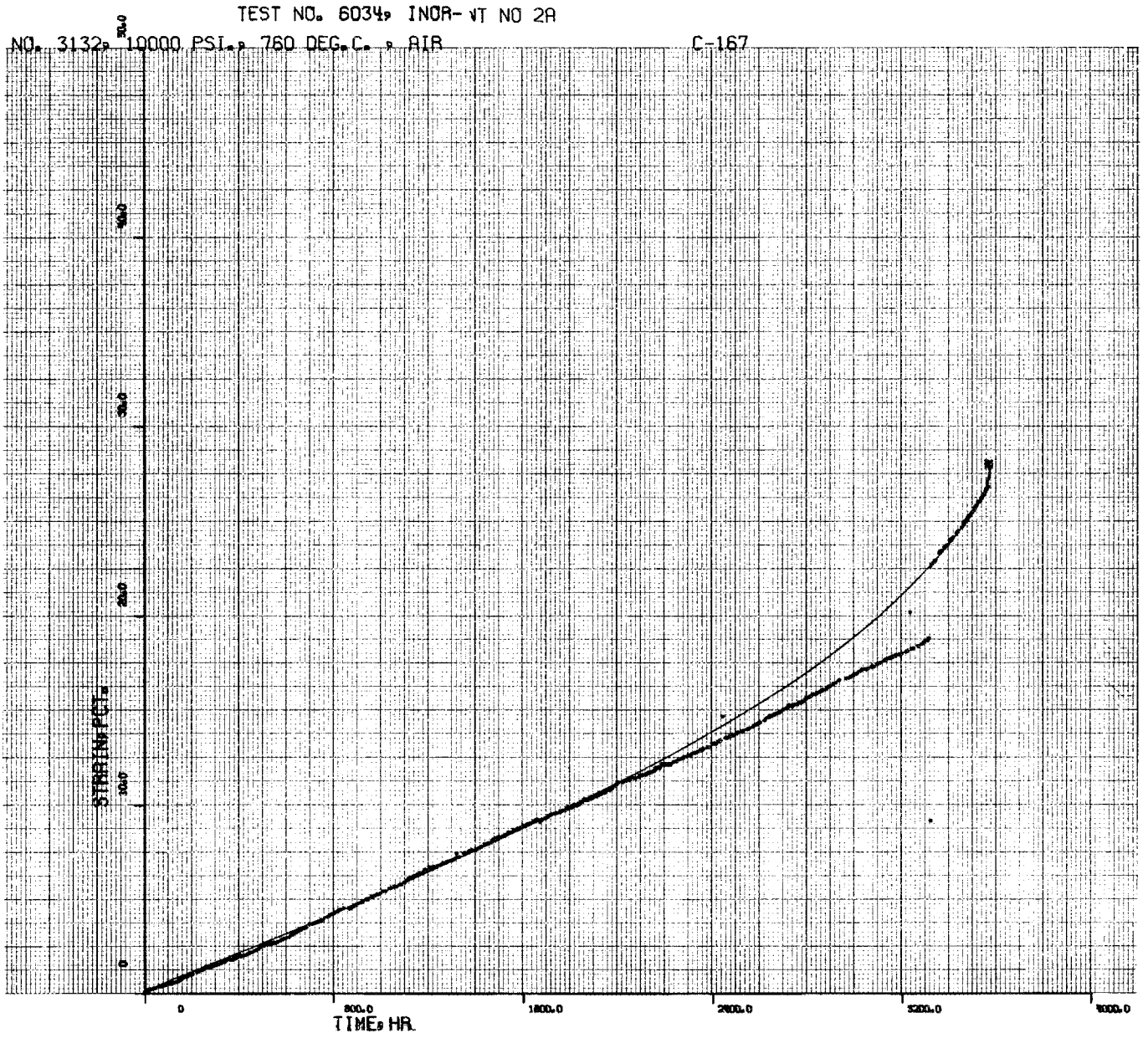

Fig. 12. Creep Curve for Test 6034.

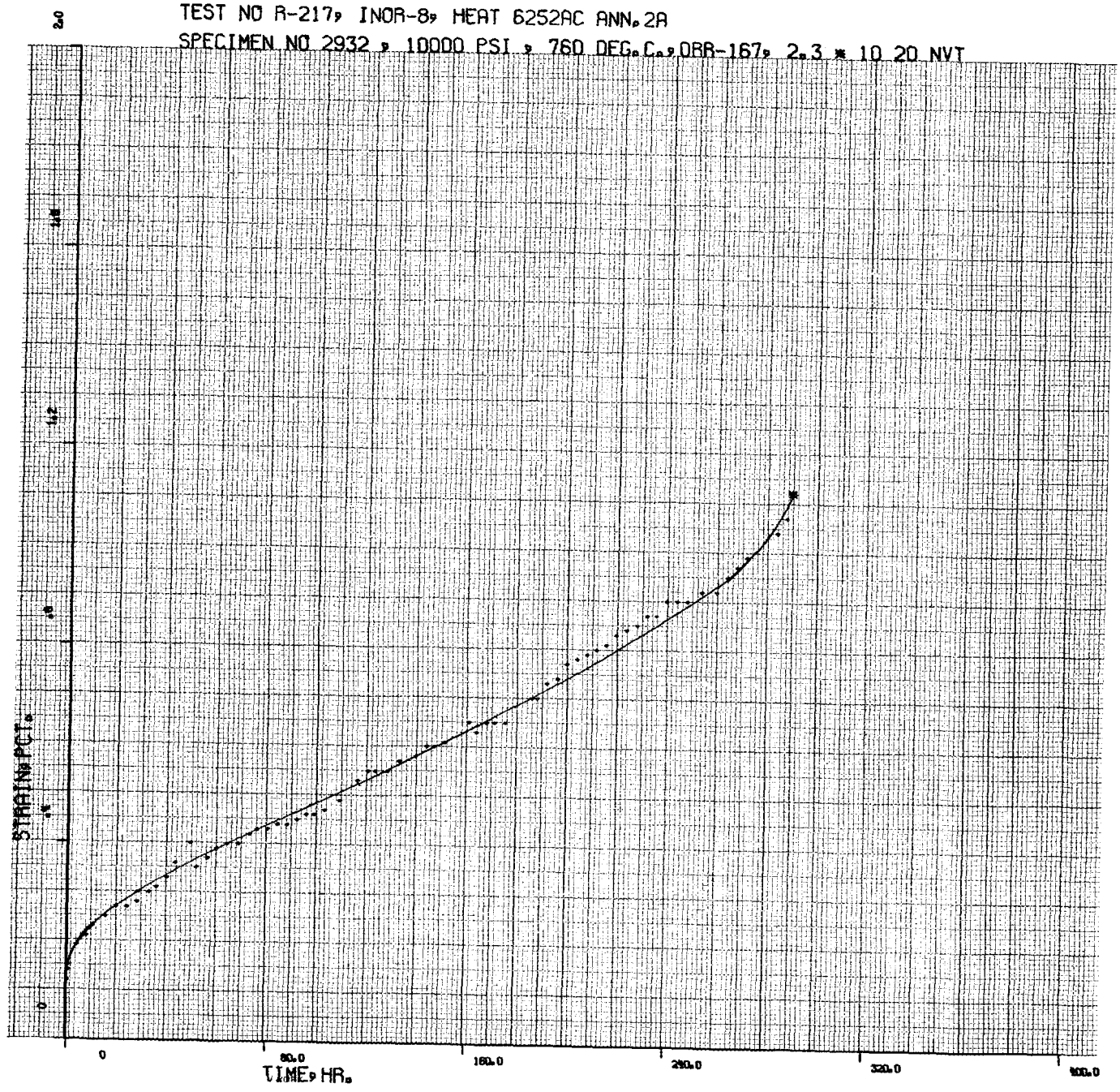

Fig. 13. Creep Curve for Test R-217.

are quite similar up to the point where the irradiated specimen failed. Figures 12 and 13 show the results of tests at 760°C and 10,000 psi on unirradiated and irradiated specimens, respectively. There is no distinguishable primary creep stage, and the results are quite comparable up to fracture of the irradiated specimen.

Since considerable data were obtained on heats 5911 AW and 5911 TH with heat treatment 1, the creep properties of these materials were examined in detail. Further details of the creep behavior are given in Table 7. At 650°C the behavior of the two lots of material was quite similar. The times for rupture and 1% strain for unirradiated and irradiated material at 650°C are compared in Fig. 14. The curve for rupture of the irradiated material falls just short of the 1% strain curve for the unirradiated specimens. At 760°C materials 5911 AW and 5911 TH have slightly different strength properties. Figure 15 shows the results for heat 5911 AW-anneal 1. At 8000 psi, the time to 1% strain for the irradiated specimen agrees very well with that for the unirradiated material. At 10,000 psi, the time to 1% strain for the irradiated material is slightly less than that for the unirradiated specimen. The data for heat 5911 TH-anneal 1 are plotted in Fig. 16. The time to 1% strain for the irradiated material is much shorter than that for the unirradiated material at high stresses, but the two nearly converge at lower stresses. This behavior agrees well with the minimum creep rate behavior shown in Fig. 8. There is some uncertainty in Fig. 16 concerning the location of the curve for the time to 1% strain. Since an extensometer was not used in the laboratory tests, the scatter in data for small strains is understandable.

In an effort to determine the effects of strain rate on the rupture ductility at 650 and 760°C, several specimens were tested in the unaged condition at various strain rates. The results of these tests are given in Table 8. The tensile results from Tables 3 and 8 and the creep results from Table 5 were used to obtain the plot of ductility versus strain rate in Fig. 17. At 650°C the ductility decreases with decreasing

Table 7. Detailed Creep Properties on Heats 5911 AW-1 and 5911 TH-1[a]

Test Number	Test Temperature (°C)	Stress (psi)	Time (hr) to Indicated Strain (%)				
			1	2	5	10	Rupture
			Heat 5911 AW-1				
6185	650	65,000	0.2	1.4	6.5	9.4	9.4
6014	650	55,000			17.5	46	49.6
6013	650	47,000	3.0	17	90	175	206.5
6012	650	40,000	31.5	80	198	351	413.7
6186	650	40,000	62	113	260	445	598.2
6059	650	32,400	195	340	774	1322	1828.1
R-194	650	47,000	7.8				12.8
R-182	650	40,000					43.0
R-170	650	32,400					144.3
6126	760	30,000	1.0	2.1	5.7	11	21.8
6187	760	25,000	2.2	5	13	26	53.7
6023	760	20,000	9.5	17	41.5	73	147.7
6039	760	17,500	15	35	97	189	367.7
6024	760	15,000	30	63	152	277	607.2
6188	760	13,000	52	110	275	525	1198.9
R-177	760	10,000	~105				104.6
R-196	760	8,000	645				834.8
			Heat 5911 TH-1				
6042	650	55,000	3	8.5	25	42	48.9
6018	650	47,000	14	40	99	166	189.1
6017	650	40,000	44	95	230	430	706.3
6056	650	32,400	260	495	1090	1750	2082.1
6125	760	30,000	1.0	2.4	6.3	12	17.7
6190	760	25,000	1.8	4.3	12	23	27.7
6029	760	20,000	8.7	16	38.5	72	113.5
6043	760	17,500	7.9	27	76	142	161.4
6030	760	15,000	52	90	202	372	654.7
R-176	760	20,000					1.0
R-184	760	15,000	~2				2.1
R-218	760	8,000	250				365.2

[a]See Tables 5 and 6 for other details.

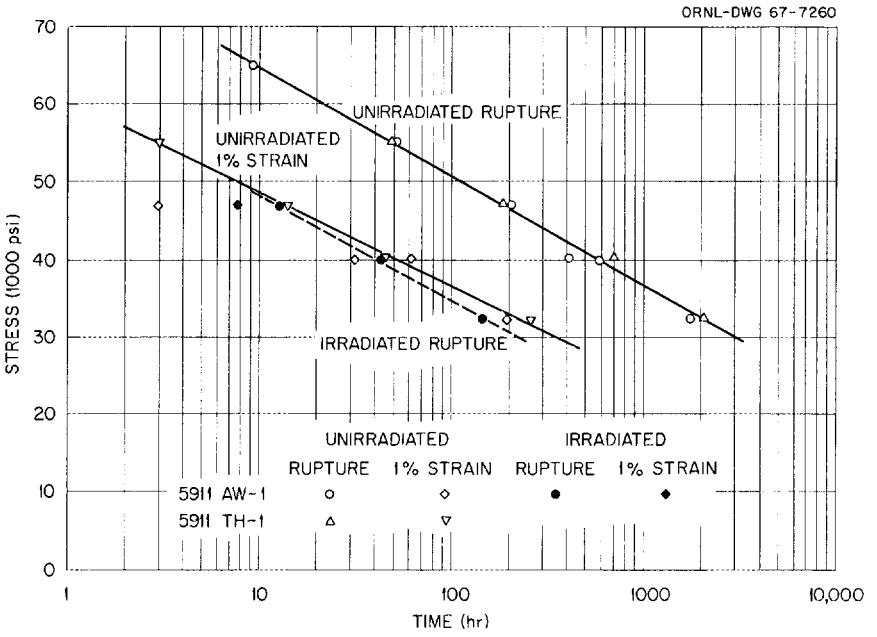

Fig. 14. A Comparison of the Unirradiated and Irradiated Creep Rupture Behavior of Heats 5911 AW-1 and 5911 TH-1 at 650°C.

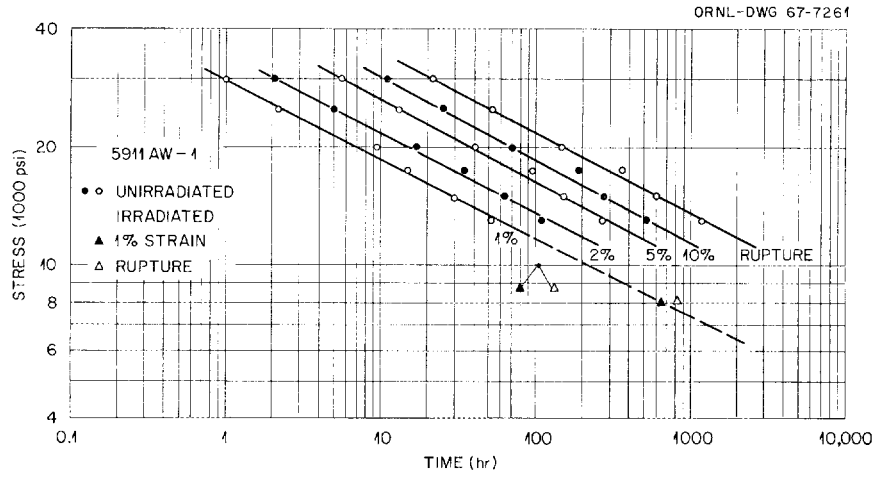

Fig. 15. A Comparison of the Creep-Rupture Properties of Heat 5911 AW-1 at 760°C in the Irradiated and Unirradiated Conditions.

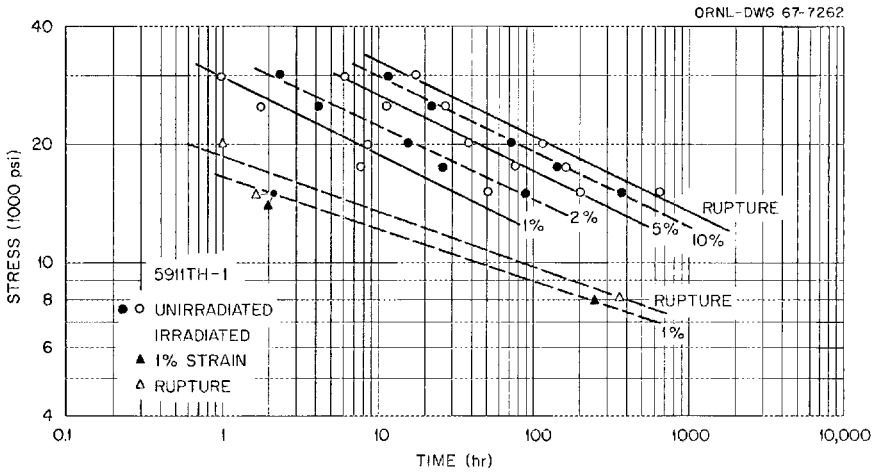

Fig. 16. A Comparison of the Creep-Rupture Properties of Heat 5911 TH-1 at 760°C in the Irradiated and Unirradiated Conditions.

strain rate. At high strain rates, the ductility is lower at 760°C than at 650°C and decreases with decreasing strain rate. A minimum is reached at a strain rate of about 10%/hr and an increase in ductility occurs as the strain rate is decreased further.

Our metallographic studies were confined to the unirradiated tensile specimens that were aged and tested at 650 and 760°C at a strain rate of 0.002 min^{-1}. The failures were all intergranular at 760°C. At 650°C extensive intergranular cracking occurred, and the failures were predominantly intergranular even though some areas failed by transgranular shear. The microstructure of a specimen from heat 5911 AW-anneal 1 after aging and testing at 650°C is shown in Fig. 18. The grain size is relatively coarse with stringers, probably of the M_6C type. The microstructure of heat 5911 AW-anneal 3 is shown in Fig. 19. The cold working and recrystallization of this material has resulted in the formation of bands of small grains and a "ghost" structure in which fine precipitates mark the boundaries of the original grains before recrystallization. The coarse microstructure of heat 5911 AW-anneal 3A is shown in Fig. 20. The "feathery" growth is probably fine carbides that have reprecipitated. These were not visible in the specimen aged at 650°C. Small amounts of the same product were visible in the other heat 5911 AW specimens that were aged at 760°C. The microstructure of heat 5911 TH-anneal 1 after aging and testing at 650°C is shown in Fig. 21. The grain

Table 8. Tensile Properties of Heat 5911 AW-1 at Various Strain Rates

Specification Number	Test Temperature (°C)	Strain Rate (min^{-1})	Stress (psi)		Elongation (%)		Reduction in Area (%)
			Yield	Tensile	Uniform	Total	
5167	650	2.0	34,200	79,500	60.1	68.6	53.4
5168	650	0.5	37,000	81,700	65.5	67.2	53.6
5169	650	0.2	26,500	80,300	55.3	57.9	40.8
5170	650	0.05	26,700	75,600	41.0	42.6	36.1
5171	650	0.02	26,300	74,000	38.9	40.5	32.4
5172	650	0.005	27,200	65,200	28.6	29.7	26.0
5173	650	0.002	26,900	61,900	26.5	27.6	23.6
5174	760	2.0	31,300	67,400	44.8	50.4	34.1
5175	760	0.5	25,900	68,300	36.5	38.4	30.6
5176	760	0.2	26,400	65,900	31.4	32.7	26.8
5177	760	0.05	26,400	62,800	26.8	28.2	20.7
5179	760	0.02	26,600	62,500	11.2	11.7	24.6
5180	760	0.005	26,000	55,600	15.6	21.9	18.4
5181	760	0.002	27,200	49,500	10.0	21.8	21.2

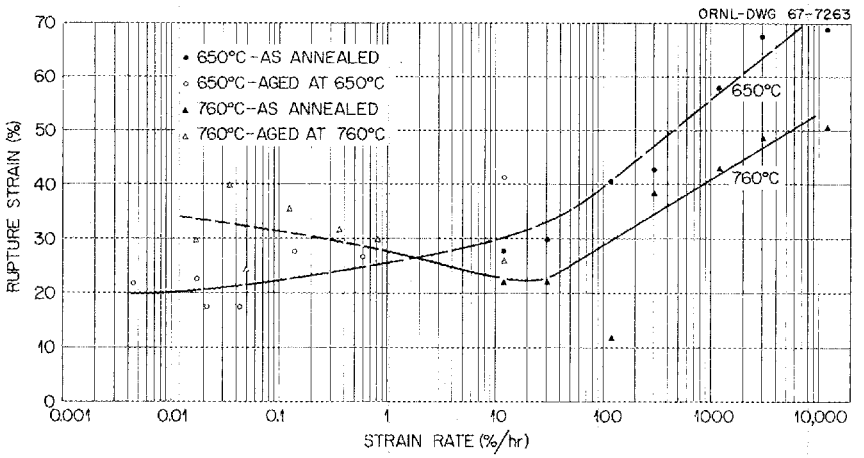

Fig. 17. Influence of Strain Rate on the Rupture Strain of Heat 5911 AW-1 at 650 and 760°C.

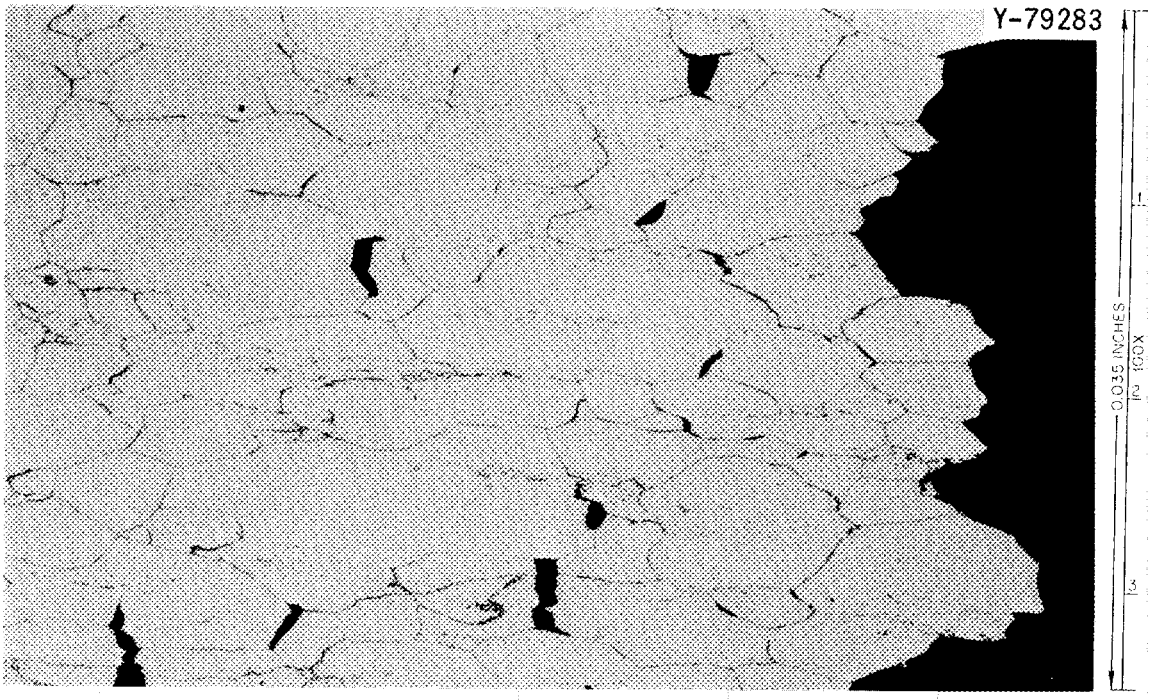

Fig. 18. Photomicrograph of the Fracture of a Heat 5911 AW-Anneal 1 Specimen Tested at 650°C at a Strain Rate of 0.002 min^{-1}. Etchant: glyceria regia.

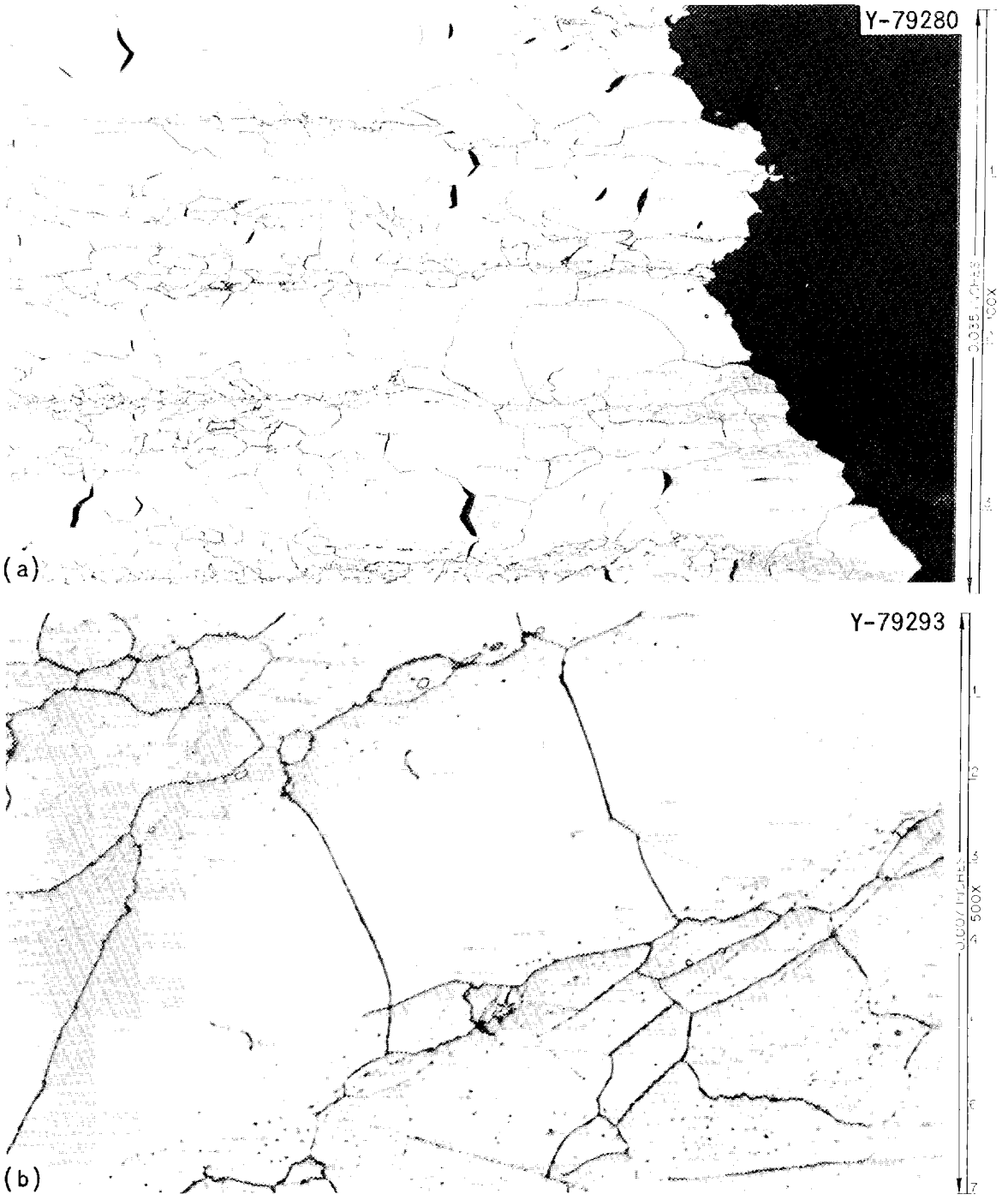

Fig. 19. Photomicrographs of a Specimen from Heat 5911 AW-Anneal 3 Tested at 650°C at a Strain Rate of 0.002 min^{-1}. Etchant: glyceria regia.

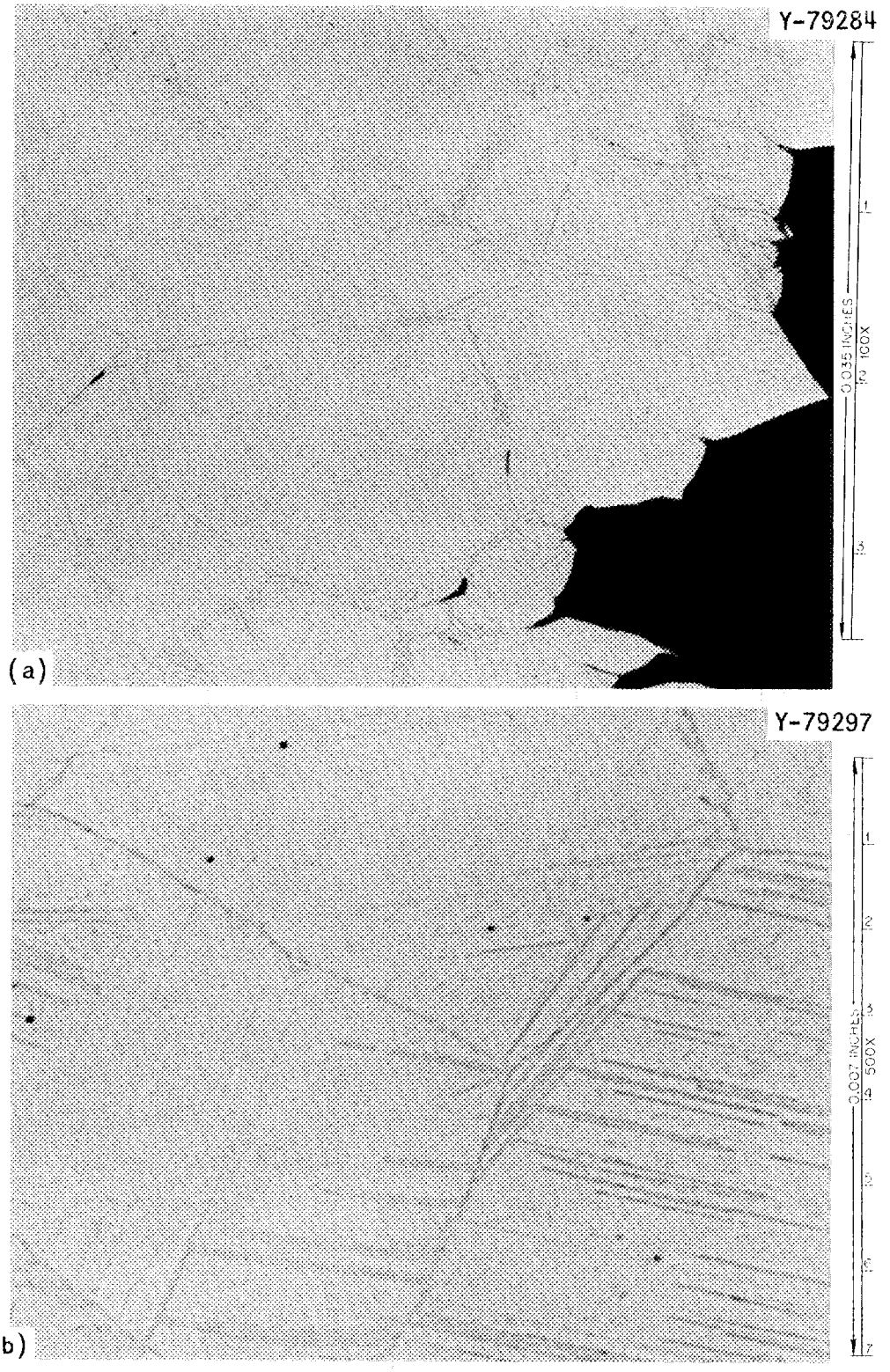

Fig. 20. Photomicrographs of a Specimen from Heat 5911 AW-Anneal 3 Tested at 760°C at a Strain Rate of 0.002 min^{-1}. Etchant: glyceria regia.

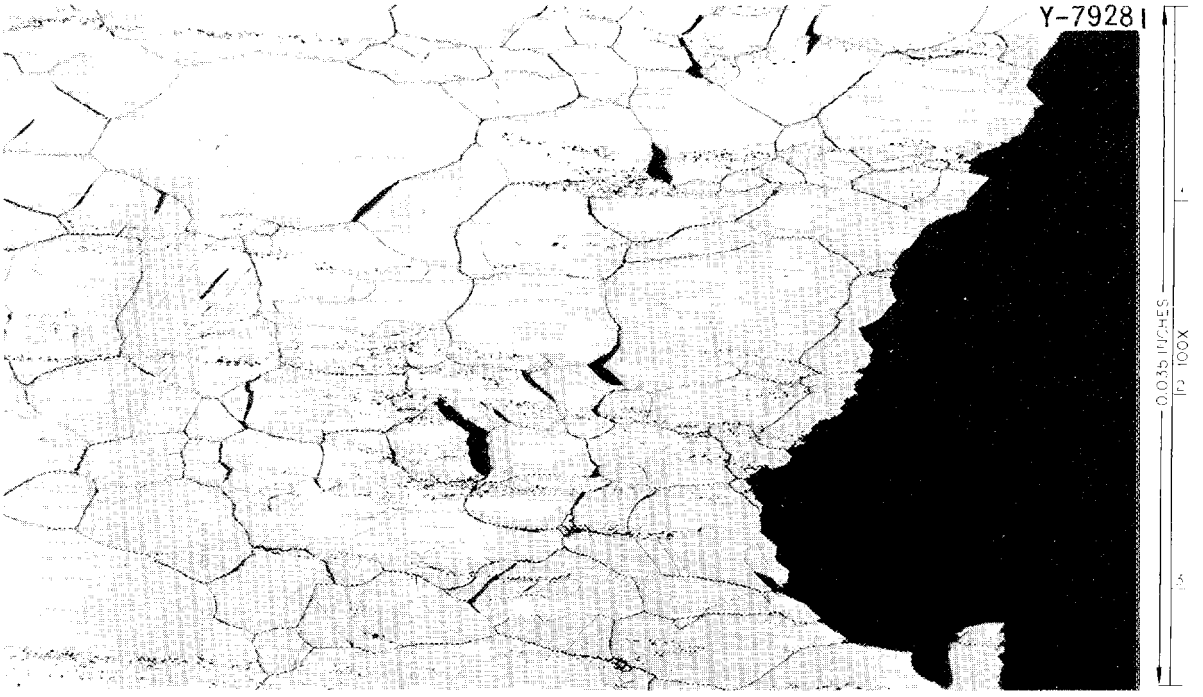

Fig. 21. Photomicrograph of the Fracture of a Specimen from Heat 5911 TH-Anneal 1 Tested at 650°C and at a Strain Rate of 0.002 min^{-1}. Etchant: glyceria regia.

size is quite similar to that of heat 5911 AW-anneal 1 (Fig. 18), but the curved twin boundaries are indicative of the more complex and extensive working of the tube hollow.

Heat 6252 AC was not homogenized adequately by any of the heat treatments used. This material was received as a section cut from an as-cast 12-in.-diam billet. Figure 22 shows the microstructure after anneal 2 and aging and testing at 650°C. A lamellar phase and the typical carbide stringers have been "smeared" through the metal in a very inhomogenous manner. Figure 23 shows that the working of treatments 2 + 3 improved the homogeneity but not sufficiently to yield a typical microstructure. Figure 24 shows that the higher temperature encountered in anneal 2A increased the grain size, but only increased the degree of segregation.

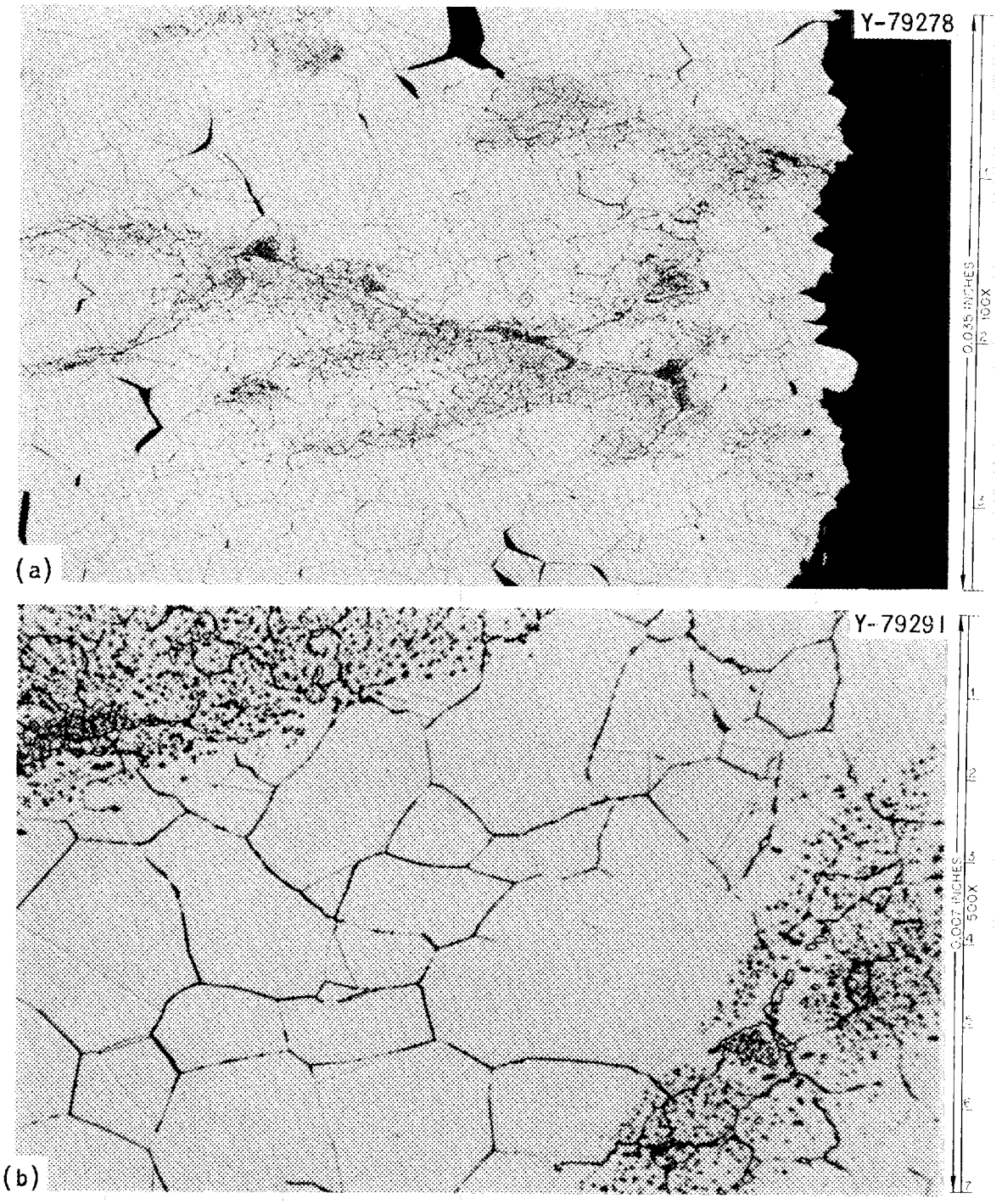

Fig. 22. Photomicrographs of a Specimen from Heat 6252 AC-Anneal 2 Tested at 650°C at a Strain Rate of 0.002 min^{-1}. Etchant: glyceria regia.

Fig. 23. Photomicrograph of the Fracture of a Specimen from Heat 6252 AC-Anneal 2 + 3 Tested at 650°C and at a Strain Rate of 0.002 min^{-1}. Etchant: glyceria regia.

Fig. 24. Photomicrograph of the Fracture of a Specimen from Heat 6252 AC-Anneal 2A Tested at 760°C and at a Strain Rate of 0.002 min^{-1}. Etchant: glyceria regia.

DISCUSSION OF RESULTS

The effects of several variables on the unirradiated properties of Hastelloy N were investigated. The dramatic decrease in tensile ductility with increasing test temperature is a characteristic of this alloy.[4] However, the exact mechanism of the ductility minimum is not understood. Our results showed that the ductility is very strain rate dependent over certain ranges of temperature and strain rate. For example, Fig. 17 shows that the rupture strain at high strain rates is greater at 650°C than at 760°C, and at low strain rates the converse is true. The changes in tensile properties as a result of varying the anneal and the aging treatment (650 or 760°C) are relatively small for such a complex alloy. Although adequate work was not done to support this conclusion, these changes are probably due to variations in grain size and the concentration and morphology of grain-boundary carbides. Under creep conditions, all the variables investigated seem to have very minor effects (Figs. 3–8). Although the results obtained on heat 6252 AC generally agreed with those for the other materials, several tests exhibited low ductility. The photomicrographs shown in Figs. 22–24 demonstrate the inhomogeneous nature of heat 6252 AC. None of the mechanical and thermal treatments were adequate to homogenize the alloy. Thus, the scatter in test results is as expected.

The main object of these experiments was to determine the properties of Hastelloy N after irradiation. Irradiation changed the properties in the following ways:

1. At 650°C the yield stress was increased and the tensile stress was decreased.
2. At 760°C the yield stress was unaffected and the tensile stress was reduced.
3. The stress-rupture life was reduced, the effect being greater at 760°C than at 650°C.
4. The minimum creep rate was unaffected at 650°C but was increased at 760°C.

---

[4]H. E. McCoy, Jr., Influence of Several Metallurgical Variables on the Tensile Properties of Hastelloy N, ORNL-3661 (August 1964).

5. The rupture strain was lowered in both tensile and creep-rupture tests, with the minimum strain occurring at a strain rate of 1 to 10%/hr.

We shall discuss each of these observations separately, after we have discussed high-temperature deformation in general terms.

At high temperatures there are at least two types of intergranular failures that are reported: (a) wedge or triple point fracture and (b) cavitation. The wedge crack forms when the stress concentration at the end of a sliding boundary is sufficient to locally exceed the fracture stress. Stroh[5,6] developed an analytical expression for the value of the critical shear stress, τ, required to form a crack under these conditions

$$\tau = \sqrt{\frac{12\gamma G}{\pi L}} , \qquad (1)$$

where

γ = the effective surface energy

G = the shear modulus,

L = the length of the sliding interface (normally taken to be the grain diameter at high temperatures).

Cavitation is a term used to describe the formation of small intergranular voids and the linking of these voids to form cracks. Numerous mechanisms have been proposed for the nucleation of these voids, however, they all require plastic deformation.[7] Once nucleated, the cavities grow by the ingress of vacancies. Balluffi and Seigle[8] developed an expression for the stability of the void under an applied stress

$$\sigma = \frac{2\gamma}{r \cos^2 \theta} , \qquad (2)$$

---

[5]A. N. Stroh, Proc. Roy. Soc. 223A, 404 (1954).

[6]A. N. Stroh, Advan. in Phys. 6, 418 (1957).

[7]P. W. Davies and J. P. Dennison, J. Inst. Metals 87, 119 (1958-59).

[8]R. W. Balluffi and L. L. Seigle, Acta Met. 5, 449 (1957).

where

σ = the applied stress,

γ = the surface tension,

r = radius of the void,

θ = the angle between the applied stress and the normal to the plane in which the void lies.

When the stress becomes less than that required to satisfy this equality, the void will decrease in size. If the stress is greater, the void will grow as rapidly as the supply of vacancies will allow.

Hull and Rimmer[9] developed an expression for the kinetics of failure by the growth of these voids due to the stress induced diffusion of vacancies along the grain boundaries. Their model assumed a constant number of void nuclei that grew as spheres. The time to rupture, t_r, was related to the applied stress, σ, and other factors

$$t_r \cong \frac{kTa^3}{4(D_g \delta_z)(\sigma - P)} \Omega \ , \qquad (3)$$

where

k = Boltzman's constant,

T = the absolute temperature,

a = the void spacing,

D_g = the atomic grain-boundary diffusion coefficient,

δ_z = the width of the grain boundary

Ω = the atomic volume,

P = the externally applied hydrostatic pressure.

Hull and Rimmer found in their experimental work with impure copper that it was necessary to allow the void spacing, a, to decrease with increasing stress in order to obtain reasonable agreement between Eq. (3) and their experimental data. The activation energy was found to be less than that for bulk diffusion, so grain-boundary diffusion was assumed to be the rate controlling process.

Although the wedge and the cavitation fractures appear distinctly different when viewed in the optical microscope, we recently performed

---

[9]D. Hull and D. E. Rimmer, Phil. Mag. 4, 673 (1959).

some work with tungsten[10] that makes us question whether they result from basically different mechanisms. The stressed tungsten specimens were fractured intergranularly and the surfaces replicated to study the details of the deformation. All of the cracks seemed to be nucleated by intergranular voids. At high stresses and relatively low temperatures, the voids linked together to form cracks that appeared wedge-shaped in the optical microscope. At low stresses and high temperatures, the voids grew to quite large sizes as voids and linked together primarily by impingement. Hence, the different appearance of cracks may be influenced more strongly by the local stress concentrations available to propagate them than by differences in the mechanism of crack nucleation. Thus, even though the cracks in the Hastelloy N specimens appear to be wedge-shaped, we should still be concerned with how voids nucleate and grow in this alloy.

Let us now consider how neutron irradiation can alter the high-temperature deformation processes in this material. When the alloy is irradiated at temperatures in excess of about one-half the absolute melting point, the atoms have high mobility and the atoms displaced by fast neutrons are able to return to their normal lattice positions. However, many experimenters have shown that structural materials irradiated even at high temperatures exhibit reduced rupture ductility when tested at elevated temperatures. This effect has been correlated with the thermal neutron exposure and more specifically with the helium that is formed by the $^{10}B(n,\alpha)$ transmutation.[11] The boron, because of its size and low solubility, is initially segregated at the grain boundaries.[12] The recoil range of the α-particle produced by transmutation is 2 μ (ref. 13) so most of the helium will lie in the proximity of the grain boundaries. The solubility of the helium in the metal is very low and most of it will be precipitated as small bubbles along the grain boundaries. The size of a spherical gas bubble must satisfy the following equality

---

[10]J. O. Stiegler, K. Farrell, B.T.M. Loh, and H. E. McCoy, Jr., Trans. ASM 60, 494 (1967).

[11]P.C.L. Pfeil, P. J. Barton, D. R. Arkell, Trans. ANS 8, 120 (1965).

[12]D. R. Harries, J. Brit. Nucl. Energy Soc. 5, 74 (1966).

[13]H. P. Meyers, Aktiebolaget Atomenergi (Sweden), Report AE-53 (May 1961).

$$P_o = \frac{2\gamma}{r_o} , \qquad (4)$$

where

P_o = the internal gas pressure,

r_o = the radius.

If a tensile stress, σ, is now applied perpendicular to the boundary in which the bubble lies, the bubble will grow to a new radius, r, and the internal gas pressure will be reduced to P.

$$\sigma + P = \frac{2\gamma}{r} . \qquad (5)$$

It can be shown that the critical stress, σ_c, that must be applied for unlimited growth to occur is given by

$$\sigma_c = 0.38\ P_o = 0.76\ \frac{\gamma}{r_o} . \qquad (6)$$

By comparing Eqs. (2) and (6), it is apparent that the applied stress to allow a bubble to grow without bound is only about one-third that required for the growth of an empty void of the same size.

Thus, the presence of helium results in the formation of small gas bubbles that can serve as void nuclei. These nuclei can grow by the stress induced migration of vacancies and the applied stress necessary for their growth is reduced by the presence of helium. Russel and Vela[14] have attempted to develop an equation similar to that of Hull and Rimmer [Eq. (3)] for predicting the time to rupture with the complicating factors of a gas in the void and lenticular growth of the voids. They obtained:

$$t_r = \frac{kTd_o}{5.4\ D\rho\delta_z\ \Omega[\sigma + (2nkT\rho/d_o) - 2\pi\gamma d_o\rho]} , \qquad (7)$$

---

[14] B. Russel and P. Vela, J. Nucl. Mater. 21, 32 (1967).

where

d_o = the bubble width perpendicular to the grain boundary,

D = the diffusion coefficient (bulk or grain boundary),

ρ = the number of bubbles per unit surface area,

n = the number of atoms within each bubble.

Although several questions have been raised about some of the assumptions on which this equation is based,[15] the factors being considered seem quite reasonable and the equation is probably valid for qualitative arguments. The temperature dependence shows up primarily in the diffusion coefficient that varies exponentially with temperature. At a given temperature, the factors that combine to determine whether a void can undergo growth are the applied stress, the gas pressure in the void, and the surface energy. These three factors appear in order in the bracketed portion of the denominator of Eq. (7).

Let us now discuss the various experimental observations that were made. The increase in the yield stress at 650°C after irradiating at 650°C was not anticipated on the basis of previous work.[16] However, the previous work involved air-melted materials irradiated at 700°C, and a direct comparison cannot be made with the results of the present study. This increase in yield stress is probably due to the formation of fine, generally dispersed precipitates during irradiation. Since 650°C is only approximately 0.55 of the absolute melting point of the alloy, there is also a possibility that some displacement defects such as dislocation loops may be present. At 760°C the yield stress is unaffected. The tensile stresses at both 650 and 760°C are reduced by irradiation. This does not reflect a basic difference in the shape of the initial portion of the stress-strain diagram for the irradiated and unirradiated specimens, but is due simply to the premature failure of the irradiated specimen before the normal tensile stress is reached.

The reduced rupture life under creep conditions is due to the effect of helium on the processes responsible for forming wedge-shaped cracks and for cavitation that we have just discussed in detail. The reason that the

---

[15]B. Russel and P. Vela, J. Nucl. Mater. 22, 234 (1967).

[16]W. R. Martin and J. R. Weir, Nucl. Appl. 1(2), 160–167 (1965).

effect is greater at 760°C than at 650°C is probably due to the greater atomic mobility at 760°C. The motion of helium to the grain boundaries, whether as atoms or small bubbles, will be quite sensitive to temperature. For example, studies by Bloom and Stiegler[17] on type 304 stainless steel have failed to disclose any bubbles in material irradiated at 650°C, but have shown that the same material irradiated at 800°C contains bubbles up to 700 A in diameter.

The convergence of the stress-rupture curves for the irradiated and unirradiated materials at low stresses can be rationalized from Eq. (2). The lower the stress, the larger a void must be to be stable. Thus, the number of void nuclei of sufficient size to undergo extensive growth is quite small in both irradiated and unirradiated materials and the deformation processes in both approach each other at low stresses.

The reduction in ductility under tensile and creep conditions is due basically to the accumulation of helium at the grain boundaries causing premature fracture. At high strain rates, such as those encountered in tensile tests, bulk deformation accounts for a large portion of the total strain. The bulk deformation characteristics do not seem to be affected significantly by irradiation at elevated temperatures and the fracture strains for irradiated materials are fairly high. As the strain rate is decreased, the conditions become more favorable for grain-boundary deformation[18] and the ductility of the irradiated material decreases rapidly. The minimum fracture strain observed in a creep test with a creep rate of 1 to 10%/hr is likely due to the worst combination of two factors: (1) low enough stress that the ratio of grain boundary to bulk deformation is fairly high and (2) high enough stress to cause many of the helium bubbles to grow. Decreasing the stress level further causes the first factor to be more detrimental and the second factor less detrimental; the rate of change of the second factor apparently being less since the ductility improves slowly with decreasing stress level.

---

[17]E. E. Bloom and J. O. Stiegler, private communication.

[18]F. Garofalo, p. 36 in Fundamentals of Creep and Creep-Rupture in Metals, Macmillan, New York, 1965.

The higher minimum creep rate of the irradiated material at 760°C is difficult to explain, particularly since the rates converge at low stresses. Since the fraction of strain due to bulk deformation increases with stress and the grain boundary contribution decreases, it would appear that bulk deformation can occur more easily in the irradiated material. However, it would seem that this would result in a decrease in the yield stress, which was not observed. Thus, this result is not presently explained.

SUMMARY AND CONCLUSIONS

We evaluated the mechanical behavior of two heats of vacuum-melted Hastelloy N in several metallurgical conditions before and after irradiation. The various mechanical-thermal treatments studied had some small effects on the tensile properties, but the creep-rupture properties were very similar.

The specimens were irradiated to a thermal dose of 2.3×10^{20} neutrons/cm^2 at temperatures of 650 and 760°C. It was found that:

1. At 650°C the yield stress was increased and the tensile stress was decreased.
2. At 760°C the yield stress was unaffected and the tensile stress was reduced.
3. The creep-rupture life was reduced, the effect being greater at 760°C than at 650°C.
4. The minimum creep rate was unaffected at 650°C but was increased at 760°C.
5. The rupture strain was lowered in both tensile and creep-rupture tests, with the minimum occurring at a strain rate of 1 to 10%/hr.

These results are consistent with our understanding of how helium introduced by the $^{10}B(n,\alpha)$ reaction should influence the properties.

ACKNOWLEDGMENTS

This study would not have been possible without the assistance of several individuals and service groups. I gratefully acknowledge the following: J. R. Weir, E. E. Bloom, and J. O. Stiegler for reviewing this report and making several useful suggestions; B. C. Williams, N. O. Pleasant, and B. McNabb for running the tensile and creep tests; V. G. Lane, E. M. Thomas, and J. C. Feltner for data processing; H. R. Tinch for metallographic work; the Metals and Ceramics Division Reports Office for preparation of the manuscript; and Graphic Arts for preparation of the illustrations.

We also are pleased to acknowledge the assistance of Atomics International in supplying the materials used in this program and the support of the Division of Space Nuclear Systems of the AEC.

INTERNAL DISTRIBUTION

1–3. Central Research Library
4–5. ORNL – Y-12 Technical Library Document Reference Section
6–25. Laboratory Records
26. Laboratory Records, ORNL RC
27. ORNL Patent Office
28. G. M. Adamson, Jr.
29. S. E. Beall
30. D. S. Billington
31. E. E. Bloom
32. E. G. Bolhmann
33. G. E. Boyd
34. R. B. Briggs
35. D. Canonico
36. E. L. Compere
37. J. E. Cunningham
38. J. H. DeVan
39. J. H Frye, Jr.
40. R. E. Gelbach
41. J. L. Gregg
42. D. G. Harman
43. W. O. Harms
44–46. M. R. Hill
47. N. E. Hinkle
48. H. Inouye
49. P. R. Kasten
50. C. R. Kennedy
51. R. T. King
52. A. P. Litman
53. E. L. Long, Jr.
54. H. G. MacPherson
55–59. H. E. McCoy, Jr.
60. C. J. McHargue
61. A. J. Miller
62. A. R. Olsen
63. P. Patriarca
64. M. W. Rosenthal
65. H. C. Savage
66. J. L. Scott
67. C. E. Sessions
68. J. Stanley
69. J. O. Stiegler
70. G. M. Slaughter
71. D. A. Sundberg
72. D. B. Trauger
73–77. J. R. Weir, Jr.
78. J. W. Woods
79. M. S. Wechsler

EXTERNAL DISTRIBUTION

80. G. G. Allaria, Atomics International
81. J. G. Asquith, Atomics International
82. D. F. Cope, RDT, SSR, AEC, Oak Ridge National Laboratory
83. H. M. Dieckamp, Atomics International
84. F. D. Haines, AEC, Washington
85. C. E. Johnson, AEC, Washington
86. W. L. Kitterman, AEC, Washington
87. W. J. Larkin, AEC, Oak Ridge Operations
88. P. J. Levine, Westinghouse Advanced Reactor Division, Waltz Mill Site, Madison, Pa.
89. A. B. Martin, Atomics International
90. D. G. Mason, Atomics International
91. G. W. Meyers, Atomics International
92. W. E. Ray, Westinghouse Advanced Reactor Division, Waltz Mill Site, Madison, Pa.
93. D. E. Reardon, AEC, Canoga Park Area Office
94. J. M. Simmons, AEC, Washington
95. S. R. Stamp, AEC, Canoga Park Area Office
96. G. A. Whitlow, Westinghouse Advanced Reactor Division, Waltz Mill Site, Madison, Pa.
97. R. F. Wilson, Atomics International
98. Laboratory and University Division, Oak Ridge Operations
99–113. Division of Technical Information Extension